Physica 2D (1981) 495–512
North-Holland Publishing Company

PSEUDOINTEGRABLE SYSTEMS IN CLASSICAL AND QUANTUM MECHANICS

P.J. RICHENS and M.V. BERRY
H.H. Wills Physics Laboratory, Tyndall Avenue, Bristol BS8 1TL, UK

Received 5 August 1980
Revised 17 November 1980

We study particles moving in planar polygonal enclosures with rational angles, and show by several methods that trajectories in the classical phase space explore two-dimensional invariant surfaces which are generically not tori as in integrable systems but instead have the topology of multiply-handled spheres. The quantum mechanics of one such 'pseudointegrable system' is studied in detail by computing energy levels using an exact formalism. This system consists of motion on a unit coordinate torus containing a square reflecting obstacle with side L. We find that neighbouring levels avoid degeneracies as L varies, and that the probability distribution for the spacing S of adjacent levels vanishes linearly as $S \to 0$ ('level repulsion'). The Weyl area rule plus edge and corner corrections gives a very accurate approximation for the mean level density. Oscillatory corrections to the mean level density are given as a sum over closed classical paths; for pseudointegrable systems these closed paths form families covering part of the phase-space invariant surfaces.

1. Introduction

In this paper we introduce a new concept into mechanics, by drawing attention to a class of Hamiltonian systems with n freedoms and n constants of motion for which, contrary to what might be expected on the basis of a theorem of Arnol'd [1], the phase flow is confined to surfaces that do not have the topology of an n-torus. We call such systems 'pseudointegrable'. Arnol'd's theorem relies on the construction of non-singular vector fields from the constants of motion, but for pseudointegrable systems we shall show that the fields have singularities, which cause the flow to lie on multiply-handled spheres.

The system we study is the motion of particles in two-dimensional polygonal enclosures whose angles are rational multiples of π. In such 'rational billiards' any trajectory can have only a finite number of directions and so the invariant surface it describes in phase space can be at most two-dimensional. A method for systematically constructing these invariant surfaces is described in section 2 and used to prove that in general they are not tori. A consequence is that no unique action variables can be defined, so that the motion cannot be integrated by a transformation to these variables [1, 2]. This is the reason for choosing the term 'pseudointegrable' for such systems. Motion in pseudointegrable systems has a chaotic property, arising not from the divergence of all pairs of neighbouring trajectories but from the splitting of beams of trajectories at certain polygon vertices. This splitting suggests that no global generating function exists that would enable the motion to be integrated by a canonical transformation, not to action-angle variables but simply to variables in which the new momenta are the constants of motion. We therefore conjecture that pseudointegrable systems are nonintegrable.

In quantum mechanics, pseudointegrability implies that the familiar 'Bohr–Sommerfeld' method cannot be employed to determine the energy levels, because this depends on the existence of tori [2, 3, 13]. We use two methods for elucidating the quantal implications of the existence of this new type of classical motion, choosing for detailed study a particular rational billiard that we call the 'square torus billiard'. This consists of a square reflecting obstacle in the centre of a unit square with periodic boun-

0167-2789/81/000–000/$02.50

dary conditions (i.e. a coordinate torus). The reason for selecting this system is in order to compare it with the superficially similar case of the Sinai billiard, where the obstacle is circular, which has been proved by Sinai [9] to give rise to *ergodic* motion (i.e. the invariant phase space surface is three-dimensional) and whose quantum mechanics has been studied in detail by Berry [4].

The first method is numerical. Using a technique developed in section 3, the energy levels of the square torus billiard are presented in section 4. By computing the probability distribution of the spacings between neighbouring levels, we show that the spectrum exhibits the property of level repulsion [4] characteristic of generic systems.

The second method is a semiclassical expansion of the density of states in terms of closed orbits, derived in section 5 by the Green function method of Gutzwiller [5] and Balian and Bloch [6]. The corresponding expansion for integrable systems, derived by Berry and Tabor [7], involves families of equivalent closed orbits covering entire phase space surfaces (tori in that case). For pseudointegrable systems the families cover only certain regions of the surfaces. Numerical computations of the closed path sum for the square torus billiard (with complex energies) gives good agreement with the density of states obtained from the exactly-computed levels of section 4.

2. Topology of classical invariant surfaces

The path geometry of a particle moving freely in an enclosure is independent of its energy. Consequently the motion can be considered as lying in a three-dimensional domain of phase space whose coordinates are position $q = (x, y)$ and path direction θ. The path lies in a sequence of replicas of the enclosure ('sheets') situated at different values of θ. Reflection at the boundary corresponds to jumping between two sheets in q, θ space.

Here we consider only enclosures with straight edges enclosing angles which are rational multiples of π. On these 'rational billiards' any path is confined to a finite number of sheets in q, θ space. To determine the topology of the continuous surface formed by sewing the sheets together, we observe that reflection at an edge is equivalent to continuing the path into a reflection of the enclosure [21] (fig. 1a). By this construction we identify the edges of every sheet and hence obtain the surface topologically equivalent to that on which the particle moves. Since the number of sheets and the size of the enclosure are finite, this surface is compact.

As a simple illustration, consider an equilateral triangular enclosure. This has six sheets, which can be sewn together to form a hexagon with edges and vertices indentified (fig. 1b); a path in the triangle is represented on this diagram as a straight line with constant direction. By joining the identified pairs a, b, c, it turns out (fig. 1c) that the phase-space surface of the equilateral triangle has the topology of a torus; therefore this system is integrable. The same argument was previously employed for this case by Keller and Rubinow [20].

In fact any polygon which tesselates the plane under the reflection rule is integrable. However, polygons which merely tesselate under a *translation* rule have motions that do not lie on tori, and are pseudointegrable if all angles are rational. (If any angle is irrational, then we conjecture that the motion is ergodic; arguments supporting this are given by Hobson [21]). Consider for example the rhombus with angles $\pi/3$ and $2\pi/3$, whose phase-space surface is shown on fig. 1d. When the indicated connections are made, the result is not a torus but a two-handled sphere (genus 2); this will be shown later. By contrast, if the same rhombus had *periodic* boundary conditions the motion would trivially lie on a torus. The difference between these two cases arises from the splitting of paths at the $2\pi/3$ vertex in the reflecting enclosure, which does not occur in the periodic 'enclosure' and

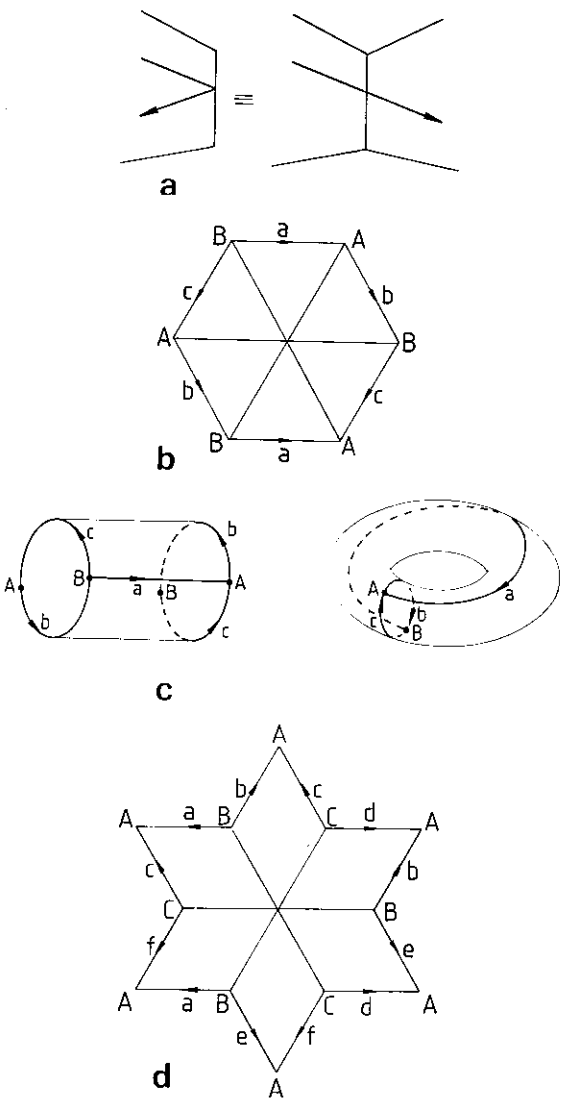

Fig. 1. (a) Illustration of the reflection rule: (b) phase-space surface of the equilateral triangle; (c) identifications made in (b) to give a torus; (d) phase-space surface of $\pi/3$ rhombus.

which leads to very different subsequent motion.

Consider now the 'square torus billiard' (fig. 2a), consisting of a torus enclosure (i.e. a square with periodic boundary conditions) containing a square reflecting obstacle. Unlike the Sinai billiard [4], which is ergodic [9], the phase-space surface of the square torus billiard consists of four sheets in q, θ space, with edges and vertices identified as in fig. 2b. The edges of the obstacle can be joined to form the 'skeleton' of a torus onto which the four sheets must be sewn. As shown in fig. 2c, and more formally later, this construction yields a five-handled sphere (genus 5).

In the square torus billiard the squares of the momentum components, p_x^2 and p_y^2, are conserved on reflection at the obstacle, so that this system possesses two constants of motion (which are, moreover, in involution). This presents us with the problem of finding the mechanism of violation of Arnol'd's theorem [1], according to which the motion would lie on a torus rather than a surface of genus 5. The solution lies in the assumption, made in the proof of Arnol'd's theorem, that two non-singular vector fields in phase space can be constructed from the constants of motion. The fact is that the vector fields constructed from p_x^2 and p_y^2 are singular at the vertices of the square obstacle, as we now explain.

Given any constant of motion $F(\boldsymbol{q}, \boldsymbol{p})$, a vector field $\boldsymbol{V}$ in phase space is constructed as follows:

$$\boldsymbol{V} = (\nabla_p F, \; -\nabla_q F). \tag{1}$$

It is easily shown [2] that $\boldsymbol{V}$ is parallel to the invariant manifold defined by specifying all the constants of motion. In the present problem, the constant p_x^2 generates the field

$$\boldsymbol{V} = 2p_x\hat{\boldsymbol{x}}, \tag{2}$$

where $\hat{\boldsymbol{x}}$ denotes the unit vector in the x direction. Fig. 3a shows this vector field near a vertex X of the obstacle, for the four sheets of the invariant surface. To sew the sheets together, each 270° sector of accessible space is first shrunk to 90° as in fig. 3b, and then the 90° sectors are joined smoothly as in fig. 3c. It is obvious that $\boldsymbol{V}$ has a singularity at X.

This singularity can be exploited to establish the topology of the invariant surface, by observing that its index, defined as the (signed) number

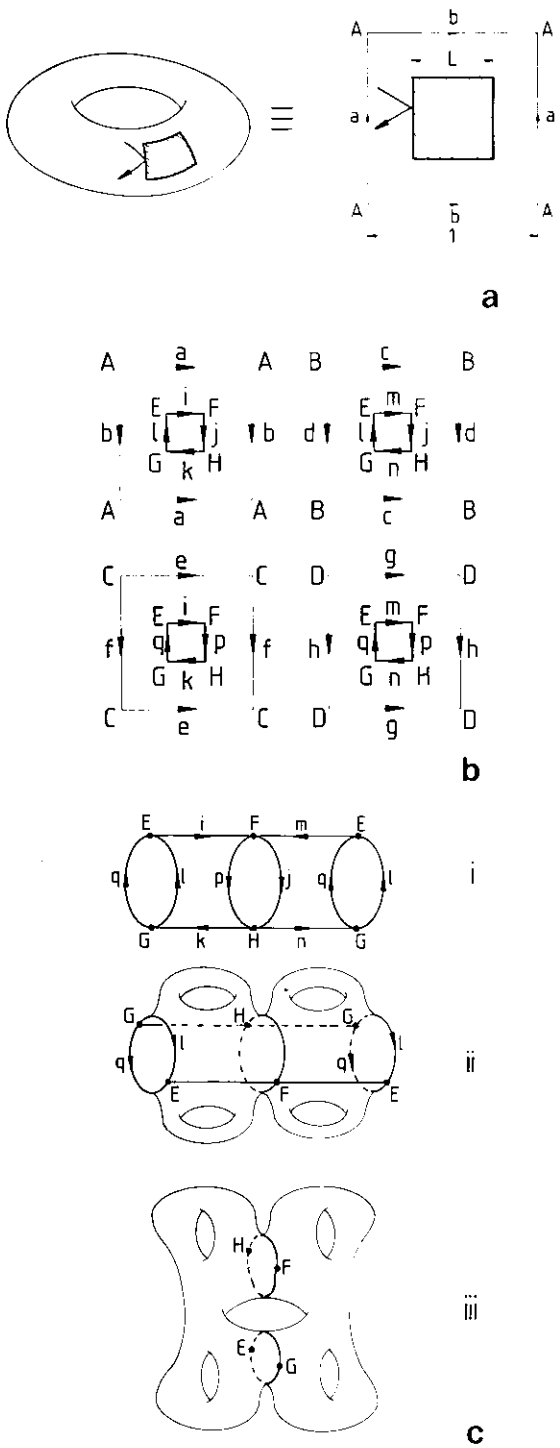

Fig. 2. (a) Equivalent representations of the square torus billiard; (b) the four phase-space sheets with edges identified; (c) construction of the five-handled sphere from (b).

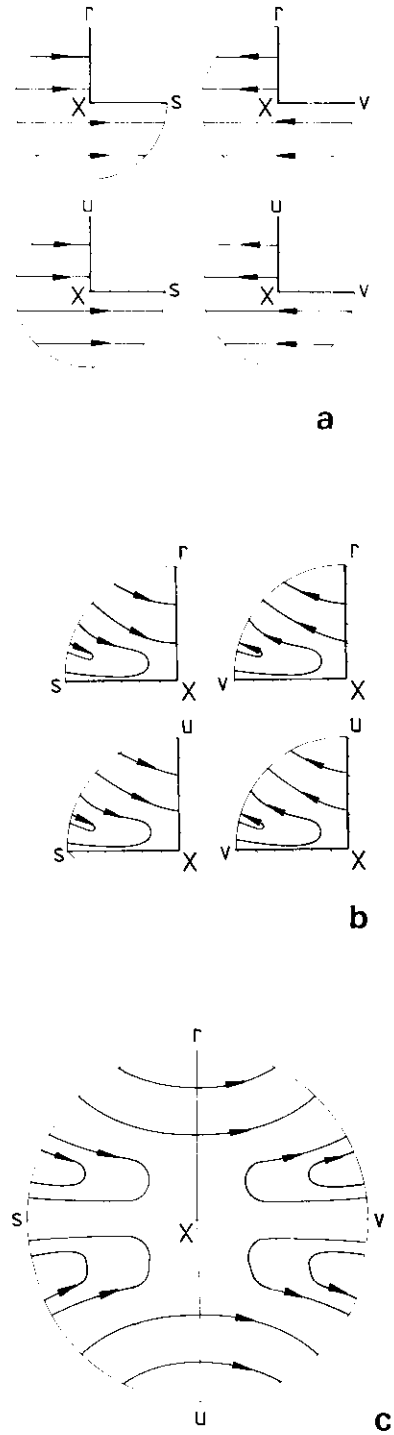

Fig. 3. (a) The vector field $V = (2p_x, 0)$ near a vertex X on the square torus billiard, for each of the four phase-space sheets; (b) deformation of (a); (c) sewing-together of the sheets in (b), displaying the singularity of index -2 at X.

of rotations of $\mathbf{V}$ during a circuit of X, is -2. The same result would be also obtained with the constant of motion p_y^2, or any combination of p_x^2 and p_y^2. Each of the four vertices has a similar singularity, so that the index $\mathcal{I}$ of the vector field over the whole invariant surface is -8. Now according to Poincaré's theorem [8], the genus g of a two-dimensional surface is related to the index $\mathcal{I}$ of a vector field on it by the relation

$$g = 1 - \tfrac{1}{2}\mathcal{I}. \tag{3}$$

For the square torus billiard, $\mathcal{I} = -8$ and so $g = 5$, as previously asserted on the basis of fig. 2. (If the vector field were nonsingular, as in Arnol'd's theorem, we would have $\mathcal{I} = 0$, so that $g = 1$ and the invariant surface would be a torus, as expected.)

Now we generalize the method just employed, to calculate the genus of the invariant surface corresponding to any rational billiard. The strategy is to obtain a contribution to the genus from each vertex by unwinding the helicoid of reflected copies of the corner, thus making it possible to determine the index of singularity of a vector field at the vertex. The vector field may be any field of constant parallel vectors on the sheets of the phase space surface.

Let the angle enclosed at a vertex be $2\pi p/q$, where q is even and the fraction p/q is otherwise in its lowest terms. We repeatedly apply the reflection rule to the edges a and b connected by this vertex, thus obtaining a helicoidal structure. In fig. 4a, b^1 is the image of b reflected in a, a^1 the image of a in b^1, b^2 the image of b^1 in a^1, etc. The condition for b^n to coincide with b is

$$4\pi n\, p/q = 2m\pi. \tag{4}$$

The helicoid then has $m(=p)$ turns and is composed of $2n(=q)$ sectors. It is now smoothly unwrapped onto the plane to see what sort of singularity of vector field has been generated. As an example consider a helicoid with 5 turns. This unwraps to give a singularity of index -4 (fig. 4b). It is not hard to see that for p turns the index is $1 - p$. The next step is to sum over all independent vertices of the polygon. If the invariant surface contains $\mathcal{N}$ sheets, a vertex will be repeated over it $\mathcal{N}/q$ times, because each helicoid contains q sectors. Consequently the genus of the surface, obtained from (3) by summing over all vertices i, is

$$g = 1 + \frac{\mathcal{N}}{2}\sum_i \frac{p_i - 1}{q_i}. \tag{5}$$

It is clear that only vertices with $p > 1$ can contribute to the extra handles that cause the invariant surface not to be a torus. For example, in the equilateral triangle of fig. 1b, all angles are $2\pi/6$ so that $p_i = 1$ and $g = 1$: as already shown on fig. 1c, the invariant surface is a torus in this case. But in the rhombus of fig. 1d two of the angles are $2\pi/3$, so that $p = 2$ and $q = 6$, and using the fact that the number of sheets is $\mathcal{N} = 6$

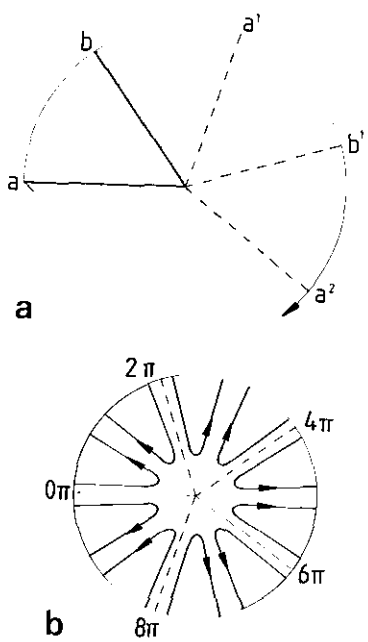

Fig. 4. (a) Reflection rule applied around a vertex; (b) map of the phase-space surface near a vertex, obtained by unwinding a helicoid with five turns.

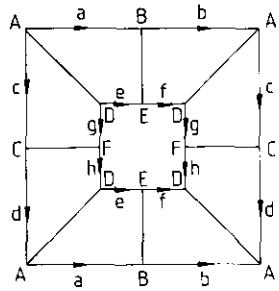

Fig. 5. Phase-space surface of the $\pi/4$ truncated triangle.

we obtain from (5) the result $g = 2$, as previously asserted. For the square torus billiard of fig. 2a there are four angles of $2\pi \times 3/4$, and four sheets, so that $p = 3$, $q = 4$, $\mathcal{N} = 4$, giving once again the result $g = 5$. Finally, we consider the truncated $\pi/4$ right triangle as shown in fig. 5, because this enclosure will play an important part in the quantum mechanics of the square torus billiard: the invariant surface has eight sheets, and there is one angle of $2\pi \times 3/8$ contributing to (5), which gives $g = 2$.

The pseudointegrability of most rational billiard systems, as embodied by the multiple-handled character of their invariant surfaces, has been established by an intuitive method based on sewing sheets together, and also by a method based on the singularities of vector fields. A third method, algebraic in character, is applied to the $\pi/3$ rhombus and the square torus billiard in appendix A.

3. Quantal formalism for square torus billiard

We have seen that for a pseudointegrable system with two freedoms, trajectories in the phase space explore a surface with g handles, where $g > 1$. Such a surface has $2g$ irreducible circuits and hence $2g$ actions, defined by

$$I = \frac{1}{2\pi} \oint \boldsymbol{p} \cdot \mathrm{d}\boldsymbol{q} \tag{6}$$

around the irreducible circuits. In general the energy will be expressible in terms of combinations of pairs of these actions in several different ways, so that any attempt to obtain the quantum-mechanical energy levels by quantizing the actions will not lead to unique results.

The square torus billiard (fig. 2) provides a good example of this. Let the torus be the unit square with periodic boundary conditions, and let the square obstacle have side L (so that $0 \leq L < 1$). Because $g = 5$ there are ten irreducible circuits but as can be seen from fig. 6 these take only four different values, namely

$$I_1 = \frac{p_x}{2\pi}, \quad I_2 = \frac{p_y}{2\pi},$$
$$I_3 = \frac{p_x(1-L)}{\pi}, \quad I_4 = \frac{p_y(1-L)}{\pi}. \tag{7}$$

If the particle has mass μ the energy levels E are given by

$$E = (p_x^2 + p_y^2)/2\mu, \tag{8}$$

where p_x and p_y are obtained by quantizing the actions in (7) as integral multiples of Planck's constant $\hbar$. But in general this procedure gives different results when applied to the pair I_1, I_2 than when applied to the pair I_3, I_4, or any of the other four pairs of actions. The only exception occurs when L is a rational fraction h/g and the

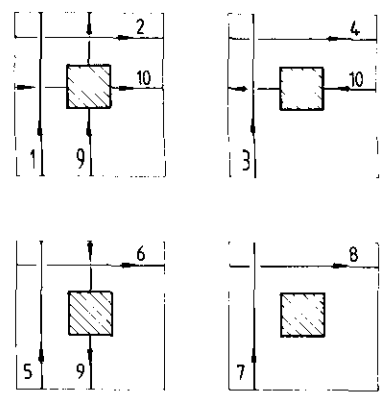

Fig. 6. Irreducible circuits of the square torus billiard.

momentum is chosen to be

$$p = 2\pi\hbar g(r, s); \tag{9}$$

in this case all four actions are quantized and the energy levels are

$$E_{m,n} = \frac{2\pi^2\hbar^2 g^2}{\mu}(r^2 + s^2). \tag{10}$$

We shall see later that this formula gives a small but finite fraction of the exact quantum levels when L is rational. In appendix B we discuss the $\pi/3$ rhombus of fig. 1d, where a similar argument yields half of the exact quantum levels.

In general, therefore, the method of quantization via actions fails for pseudointegrable systems. We present now a formalism yielding the exact quantal levels for the square torus billiard; the formalism can undoubtedly be generalised to other rational billiard systems but we do not pursue this here.

The eigenfunctions $\psi(x, y)$ must satisfy Schrödinger's equation

$$\frac{\partial^2\psi}{\partial x^2} + \frac{\partial^2\psi}{\partial y^2} + k^2\psi = 0, \tag{11}$$

where

$$k \equiv \sqrt{(2\mu E)}/\hbar \tag{12}$$

and the eigenvalues k or E are determined by the conditions that ψ must have the periodicity of the unit square lattice and vanish on the square boundary of the central obstacle. Most of the resulting eigenvalues are degenerate, corresponding to eigenstates related by reflection about the x axis or the square diagonal. It will prove convenient to remove these degeneracies by restricting our attention to states where ψ is odd under reflection about these two lines, as shown schematically in fig. 7a. The resulting 'desymmetrized' square torus billiard problem is equivalent to finding waves ψ that vanish on the boundary of the truncated $\pi/4$ triangle enclosure shown in fig. 7b.

We begin by expanding ψ as a sum over solutions of (11) in a semi-infinite strip of width $\Delta = \frac{1}{2}(1 - L)$, i.e.

$$\psi(x, y) = \sum_{n=1}^{\infty} a_n \sin\frac{n\pi x}{\Delta} \sin\rho_n(k)\pi y, \tag{13}$$

where

$$\rho_n(k) = \left\{\left(\frac{k}{\pi}\right)^2 - \left(\frac{n}{\Delta}\right)^2\right\}^{\frac{1}{2}}. \tag{14}$$

This is a nontrivial expansion because when $n > k\Delta\pi$ the quantities ρ_n are imaginary and the component waves grow exponentially with y. Now ψ must be constrained to vanish along the diagonal $y = x + L/2$, i.e.

$$\psi(x, x + \tfrac{1}{2}L) = \sum_{n=1}^{\infty} a_n \sin\frac{n\pi x}{L} \sin\{\rho_n(k)\pi(x + \tfrac{1}{2}L)\} = 0. \tag{15}$$

This function of x can be expanded into a

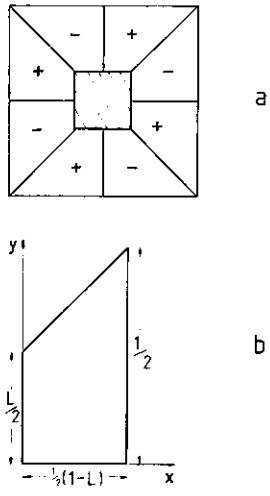

Fig. 7. (a) Desymmetrization of the square torus billiard; (b) enclosure for which the spectrum of fig. 8 was computed.

Fourier sine series,

$$\psi(x, x+\tfrac{1}{2}L) = \sum_{m=1}^{\infty} A_m \sin\frac{m\pi x}{\Delta}, \tag{16}$$

whose coefficients must all vanish identically. Some algebra gives

$$A_m = \frac{4\Delta m}{\pi}\sum_{n=1}^{\infty} a_n\rho_n(k)n \times\left\{\frac{(-1)^{m+n}\cos\tfrac{1}{2}\pi\rho_n(k) - \cos\tfrac{1}{2}\pi\rho_n(k)L}{\Delta^4\rho_n^4(k) - 2\Delta^2\rho_n^2(k)(m^2+n^2) + (n^2-m^2)^2}\right\} = 0 \tag{17}$$

This has the form

$$\sum_{n=1}^{\infty} a_n M_{nm}(k) = 0 \tag{18}$$

and can have nontrivial solutions for the expansion coefficients only if the determinant of M_{nm} vanishes, i.e. if

$$\det_{nm}\left\{\frac{(-1)^{m+n}\cos\tfrac{1}{2}\pi\rho_n(k) - \cos\tfrac{1}{2}\pi\rho_n(k)L}{\Delta^4\rho_n^4(k) - 2\Delta^2\rho_n^2(k)(n^2+m^2) + (n^2+m^2)^2}\right\} = 0. \tag{19}$$

The roots of this equation give the eigenvalues k of the desymmetrized quantal square torus billiard. Numerical results will be presented and discussed in section 4. Analytically, the claim that when L is rational some levels are given by (10) can be justified by substituting $k^2 = 4\pi^2 g^2(r^2+s^2)$ into (19) and observing that the matrix elements in the $n = (g-h)r$'th row are proportional to those in the $n = (g-h)s$'th row, so that the determinant vanishes.

4. Energy levels of the square torus billiard

By inspecting computed values of the determinant (19), the first fifty eigenvalues, expressed in terms of the variable

$$\mathscr{E} \equiv k^2/\pi^2, \tag{20}$$

where obtained as functions of the obstacle size L. The resulting spectrum of the desymmetrized square torus billiard is displayed in fig. 8.

Its most striking feature is the absence of degeneracies when L is not rational. When L is rational some degeneracies do occur, between the states (10), because of the fact that certain integers can be written as the sum of two squares in more than one way, as discussed in detail by Berry [4]. But these are rare: when $L = 0$ the lowest degenerate level is at $\mathscr{E} = 260$, and when L is non-zero the lowest degenerate level is at $\mathscr{E} = 1040$ (for $L = 1/2$). For other values of L no degeneracies were found, despite

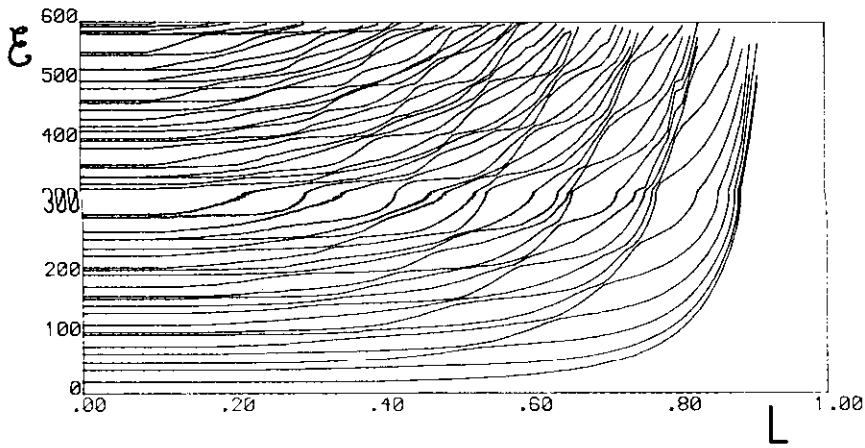

Fig. 8. Eigenvalues $\mathscr{E}$ of the square torus billiard as a function of L.

a careful search in each region where two levels came close together.

In view of a theorem of Von Neumann and Wigner [14] and Arnol'd [1], according to which the levels of a typical quantum system do not degenerate when just one parameter is varied, this absence of degeneracies shows that pseudointegrable systems display generic quantum-mechanical behaviour. In this respect they resemble ergodic systems (e.g. Sinai's billiard [4]). In an integrable system, on the other hand, degeneracies occur when a single parameter is varied [4], and the occasional degeneracies when L is rational can be regarded as the remnants of integrability as embodied in the behaviour of the four actions (7) in these special cases.

The prevalence of near-degeneracies can be quantified by the level spacing distribution $P(S)$, which is the probability density that neighbouring levels will have spacing S (normalized so that the mean level spacing is unity). $P(S)$ for the spectrum of fig. 8 is shown in fig. 9. It is clear that the function vanishes as $S \to 0$, indicating 'level repulsion'. Moreover the curve near $S = 0$ is consistent with the linear behaviour predicted by Berry [4] for generic quantum systems and found to occur for Sinai's billiard [4] and the 'stadium' [15]. This contrasts with the behaviour of integrable systems, for which $P(S) \to$ constant as $S \to 0$ [4, 16].

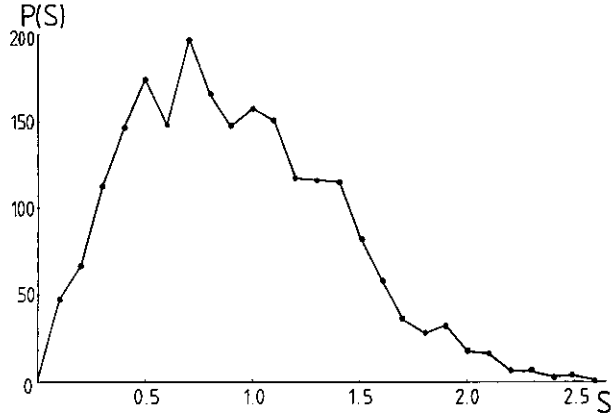

Fig. 9. Level spacing distribution for the square torus billiard.

Degeneracies and near-degeneracies describe the 'texture' of the spectrum on the finest scales of energy. To describe other features of the spectrum we first define the mode number $\mathcal{N}(\mathscr{E})$ as the number of levels with energies less than $\mathscr{E}$, i.e.

$$\mathcal{N}(\mathscr{E}) \equiv \sum_{i=1}^{\infty} \Theta(\mathscr{E} - \mathscr{E}_i), \tag{21}$$

where Θ is the unit step function and i labels the levels in order of increasing energy. The coarsest feature of the spectrum is the average mode number $\overline{\mathcal{N}}(\mathscr{E})$, obtained by smoothing the steps in $\mathcal{N}(\mathscr{E})$. For billiards, $\overline{\mathcal{N}}(\mathscr{E})$ is given by the Weyl area rule plus edge and corner corrections, as explained by Baltes and Hilf [10]. When applied to the desymmetrized enclosure of fig. 7b, this gives

$$\overline{\mathcal{N}}(\mathscr{E}) = \frac{\pi}{32}\mathscr{E}(1-L^2) - \frac{\sqrt{\mathscr{E}}}{4}\left(1 + \frac{1-L}{\sqrt{2}}\right) + \frac{11}{36}. \tag{22}$$

As shown on fig. 10 for two typical values of L, this formula gives a very accurate fit to the exact spectrum, whereas the first term alone (Weyl area rule) does not.

5. Semiclassical closed path sum

We now understand the spectrum of the square torus billiard on the smallest and largest energy scales. On intermediate scales, the distribution of energy levels is described by oscillatory corrections to the average mode number $\overline{\mathcal{N}}(E)$. In this section we shall work not with the mode number but with its derivative, the level density $d(E)$, which we write in the form

$$d(E) \equiv \frac{\mathrm{d}\mathcal{N}(E)}{\mathrm{d}E} = \sum_{i=1}^{\infty} \delta(E - E_i) = \frac{\mathrm{d}\overline{\mathcal{N}}E)}{\mathrm{d}E} + d_{\mathrm{osc}}(E). \tag{23}$$

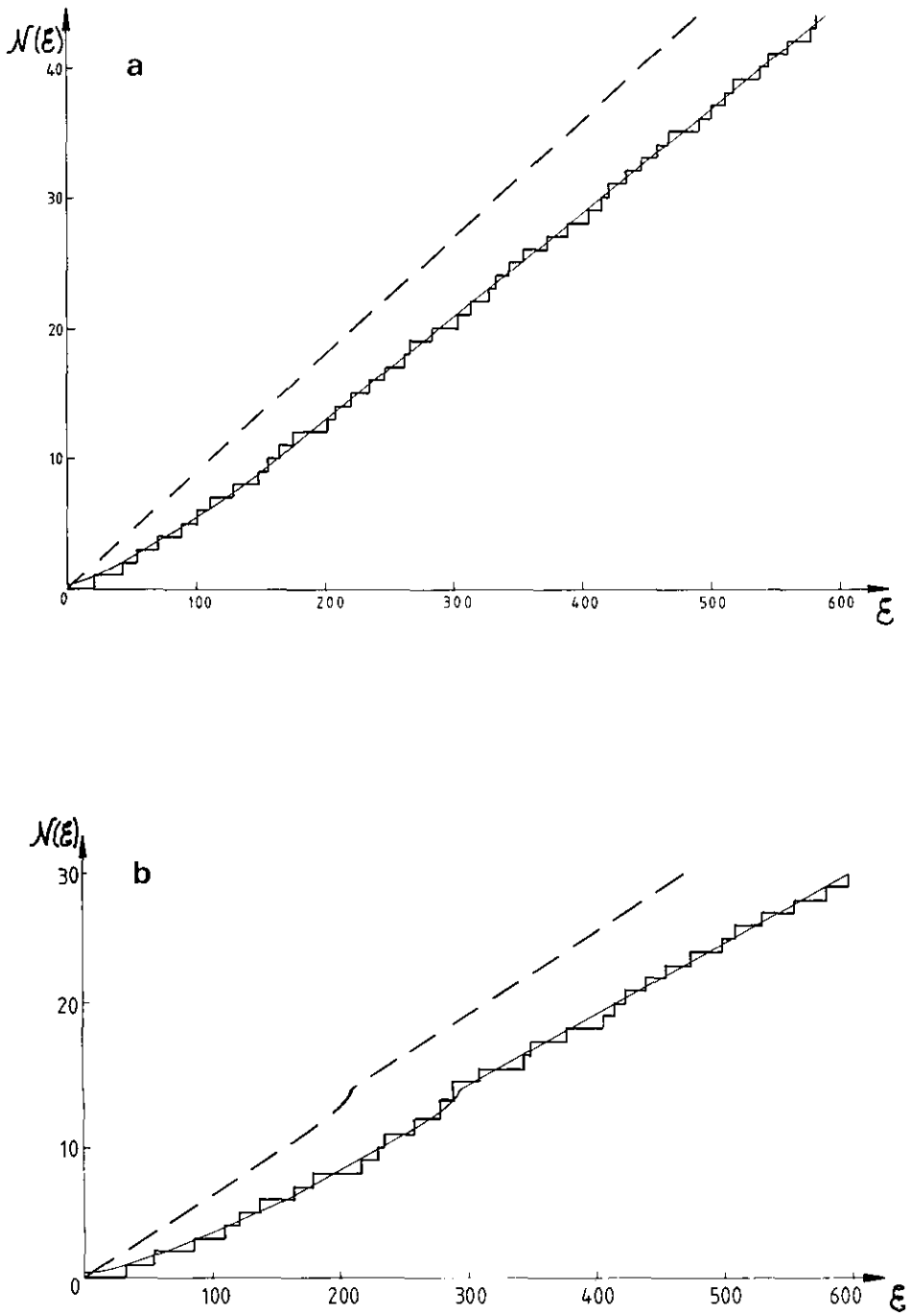

Fig. 10. Comparison of smoothed mode number $\bar{N}(\mathscr{E})$ with exact $N(\mathscr{E})$ (stepped curve) for (a) $L = 0.3$, (b) $L = 0.6$. The Weyl area rule alone is shown by dashed lines.

To find the oscillatory corrections $d_{\rm osc}$, we represent $d(E)$ in terms of the time-dependent Green function $K(q_B, q_A; t)$, as follows [11]:

$$d(E) = \frac{1}{\pi\hbar}\,\mathrm{Re}\int_0^\infty \mathrm{d}t\, \mathrm{e}^{\mathrm{i}Et/\hbar}\iint \mathrm{d}q K(q, q; t). \qquad (24)$$

To obtain a semiclassical expansion of $d_{\rm osc}$, we employ the following semiclassical approximation to K [11]:

$$K(q_B, q_A; t) \approx \frac{1}{2\pi\mathrm{i}\hbar}\sum_j \left|\frac{\mathrm{d}p_{A,j}}{\mathrm{d}q_B}\right|^{1/2} \times \exp\left\{\mathrm{i}\left(\frac{S_{AB,j}(t)}{\hbar} + \alpha_j\pi\right)\right\}. \qquad (25)$$

In this formula, j labels the classical trajectories connecting q_A and q_B in time t. The jth path has action $S_{AB,j}(t)$ leaves q_A with momentum $p_{A,j}$ and suffers α_j specular reflections at the boundary of the enclosure. For later reference we note that if the reflection boundary condition is of Neumann (rather than Dirichlet) type, that is if the normal derivative of ψ (rather than ψ itself) vanishes on the boundary, then α_j must be set equal to zero. It is easy to show that for the billiard problems with which we are concerned, the Jacobian determinant in (25) is

$$\left|\frac{\mathrm{d}p_{A,j}}{\mathrm{d}q_B}\right| = \left(\frac{\mu}{t}\right)^2, \qquad (26)$$

and the action is

$$S_{AB,j}(t) = \mu\mathscr{L}_j^2/2t, \qquad (27)$$

where $\mathscr{L}_j$ is the length of the jth orbit.

The integral over t in (24) can be now evaluated exactly in terms of Bessel functions of the third kind (Hankel functions) [17], to give

$$d(E) \approx \frac{\mu}{2\pi\hbar^2}\,\mathrm{Re}\sum_j \iint \mathrm{d}q H_0^{(1)}\left\{\frac{\mathscr{L}_j}{\hbar}\sqrt{(2\mu E)}\right\} \times \exp\{\mathrm{i}\alpha_j\pi\}. \qquad (28)$$

j now labels the classical paths (consisting of straight line segments joined by specular reflection at the boundary) which begin and end at q. These are of three types. First, there is the path of zero length; it is well known [11] that this gives the (nonoscillatory) Weyl area contribution $\mathrm{d}\bar{N}/\mathrm{d}E$ to the level density, which we have already considered in section 4. Secondly, there are the paths which intersect themselves at q, i.e. which close in position but not in momentum, and so are not periodic. For such paths, $\mathscr{L}_j$ varies with q and neighbouring contributions to the integral in (28) cancel [5, 11] as a result of destructive interference between the rapid oscillations of the Bessel function in the semiclassical limit $\hbar \to 0$, so that these paths do

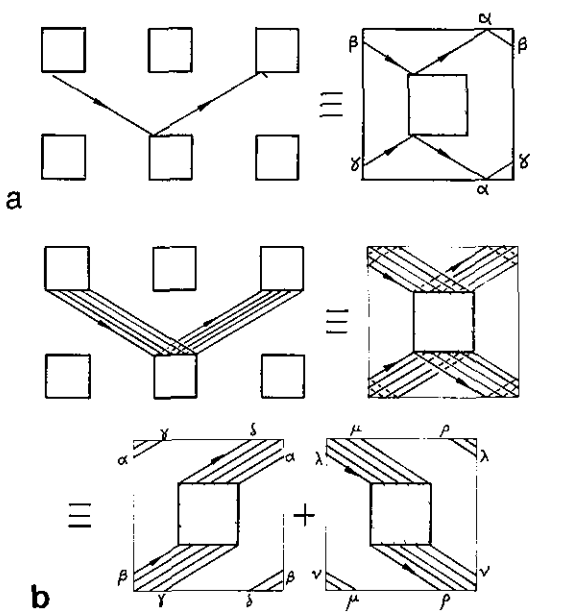

Fig. 11. (a) Closed orbit in the square torus billiard; (b) family of similar orbits forming a band on the phase-space surface.

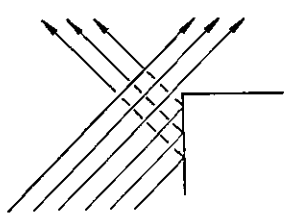

Fig. 12. Bifurcation of trajectories at a vertex.

not contribute to $d(E)$. And thirdly, there are the completely closed orbits, which pass repeatedly through q; these give rise to $d_{\rm osc}(E)$, as we now explain.

In pseudointegrable systems, as in integrable systems, the closed orbits are not isolated but form continuous families on the invariant phase-space surface. Each orbit in the family has the same value of $\mathcal{L}_j$, which is therefore independent of q, thus making trivial the integration in (28). For integrable systems each family of orbits fills its invariant surface, as explained by Berry and Tabor [7, 12]. But in a pseudointegrable system the family fills a band only partially covering the surface, as shown by the example in fig. 11. On the coordinate space this band may self-intersect, as shown by the first picture in fig. 11b. The contribution to the integral in (28) is correctly taken into account by including all branches separately, so that the family contributes a factor $\mathcal{A}_j$ equal to the area occupied by the band or orbits on the phase space surface, as shown on the second picture in fig. 11b. Thus the oscillatory part of (28) becomes, on using the asymptotic form [17] of the Bessel function,

$$d_{\rm osc}(E) \approx \left(\frac{\mu}{2\pi^2\hbar^2}\right)^{3/4} E^{-1/4} \times \sum_j \frac{\mathcal{A}_j}{\sqrt{\mathcal{L}_j}} \cos\left\{\frac{\mathcal{L}_j}{\hbar}\sqrt{(2\mu E)} + (\alpha_j - \tfrac{1}{4})\pi\right\}, \tag{29}$$

where j now labels the families of topologically different closed orbits of nonzero length. In terms of the energy variable $\mathscr{E}$, this formula becomes

$$d_{\rm osc}(\mathscr{E}) = d_{\rm osc}(E)\frac{{\rm d}E}{{\rm d}\mathscr{E}} = \frac{1}{2\sqrt{2}}\,\mathscr{E}^{-1/4} \times \sum_j \frac{\mathcal{A}_j}{\sqrt{\mathcal{L}_j}} \cos\{\pi\mathcal{L}_j\sqrt{\mathscr{E}} + (\alpha_j - \tfrac{1}{4})\pi\}. \tag{30}$$

From this result it is clear that each closed orbit contributes an oscillation to $d(\mathscr{E})$, and so describes the clustering of levels on a particular scale, which gets finer as the length of the orbit increases. The general theory of such path sums was worked out by Gutzwiller [5] and Balian and Bloch [6]; the form of the path sum for generic integrable systems was derived by Berry and Tabor [7, 12]; and the explicit expression for the path sum in a particular ergodic system (Sinai's billiard), where some closed orbits lie in families and some are isolated, was obtained by Berry [4].

In order to evaluate the path sum (30), it is necessary to enumerate the closed orbits and determine the areas of the bands they fill. The bands are bounded by orbits which strike a vertex (fig. 11). A beam of parallel trajectories containing one which is aimed at a vertex will bifurcate when it hits that vertex (fig. 12). One's first thought is that repeated such bifurcations would cause the closed orbit topologies to proliferate rapidly with increasing length. This would lead to the conclusion that the number $N(\mathcal{L}){\rm d}\mathcal{L}$ of closed orbits with lengths between $\mathcal{L}$ and $\mathcal{L} + {\rm d}\mathcal{L}$ should increase exponentially as $\mathcal{L} \to \infty$. In fact, however, careful analysis shows that the condition of specularity prevents most of these bifurcations from yielding closed orbits, and $N(\mathcal{L})$ increases much more slowly than exponentially. A detailed study of the asymptotics of $N(\mathcal{L})$ will be published later.

The path sum (30) was evaluated for the desymmetrized square torus billiard by including the first 225 closed orbits (not including repetitions) which were found by inspection. To make the series coverge, a complex energy $\mathscr{E} + i\delta$ was employed, which causes each closed-orbit contribution to acquire a factor $\exp\{-\pi\mathcal{L}_j\delta/2\sqrt{\mathscr{E}}\}$. The result is a semiclassical approximation to a smoothed level density function where the delta functions in (23) are replaced by δ-broadened Lorentz resonances [6, 7], i.e.

$$d_\delta(\mathscr{E}) = \sum_j \frac{\delta/\pi}{(\mathscr{E} - \mathscr{E}_j)^2 + \delta^2}. \tag{31}$$

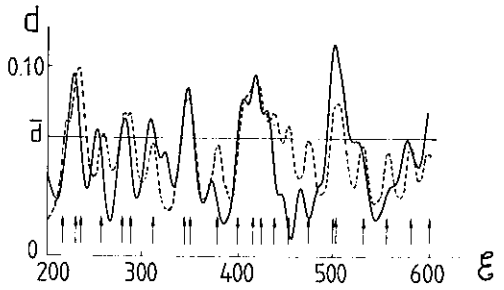

Fig. 13. Smoothed semiclassical expansion of the level density (full line) for complex energies $\mathcal{E} + i7.5$, including 225 topologies of closed orbit, compared with exact smoothed level density (dashed line), for $L = 0.6$. Positions of the exact quantum levels are marked with arrows.

Fig. 13 shows the results of the computation for $L = 0.6$ with a smoothing of $\delta = 7.5$ (the mean level spacing, obtained from (22), is 15.9 in this case). It is clear that the semiclassical closed path sum gives a quite good approximation to the exact smoothed level density. To our knowledge this is the first numerical test of a closed path expansion for the quantal spectrum of a system conjectured to be classically nonintegrable, although for the anisotropic Kepler system (which is conjectured to be ergodic) Gutzwiller has recently [19] evaluated the closed path sum by a partially analytic procedure.

Finally, we note that the bounce nuber α_j occurring in the phase of d_{osc}, eq. (30), is always even for the families of closed orbits occurring in polygonal enclosures. The reason is that any closed orbit with α_j odd will be isolated (rather than forming part of a family) because the beam of parallel orbits surrounding it will form a Möbius strip in phase space on account of the reversal of orientation on each reflection. (A simple example of this behaviour is the equilateral triangle orbit in an equilateral triangle enclosure.) This evenness of α_j has the curious implication that for polygonal billiards, including all pseudointegrable systems, the semiclassical formula (30) predicts the same spectrum for both Dirichlet and Neumann boundary conditions. The explanation, elaborated in appendix C for the integrable case of the $\pi/4$ right triangle, is that while Neumann boundaries introduce extra states (corresponding to a positive sign in 'edge' corrections to $\overline{N}(\mathcal{E})$ in for example eq. (22)), these extra states are of zero measure amongst all the states and their semiclassical closed path sum is order $\mathcal{E}^{-1/2}$ in d_{osc} rather than $\mathcal{E}^{-1/4}$ as in (30). This failure to discriminate boundary conditions does not occur for nonpolygonal billiards, as can be seen from the case of the circular enclosure for which there are equal numbers of closed orbit families with α_j even and α_j odd.

6. Conclusions

Pseudointegrable systems with two freedoms, exemplified by billiards in rational polygon enclosures, differ from ergodic systems in possessing the property, which they share with integrable systems, that the motion of trajectories in phase space is restricted to two-dimensional invariant surfaces. But these invariant surfaces are not tori as in the case of integrable systems; instead, their topology is that of multiply-handled spheres. Pseudointegrable systems are not to be confused with quasi-integrable systems, which are smooth perturbations of integrable systems [2] where most of the phase space is filled with tori while some orbits explore three-dimensional regions of small but finite measure in a hyperbolically chaotic fashion. Nevertheless, pseudointegrable motion on the multiply-handled surfaces does have a certain chaotic character, resulting not from the divergence of neighbouring trajectories but from the bifurcation of beams of trajectories hitting polygon vertices.

In quantum mechanics, it appears from the example of the square torus billiard that pseudointegrable systems possess the generic property that on the finest scales their energy levels avoid degeneracies as a parameter varies, and so their spacings exhibit level repulsion. In this respect pseudointegrable systems differ from

integrable systems and resemble ergodic ones. On the coarsest energy scales, the average level density agrees with the predictions of the Weyl area rule plus corrections, but this result holds irrespective of the nature of the classical motion. The unique character of pseudointegrable motion manifests itself quantally on intermediate scales of energy, in long-range correlations between levels as embodied in oscillatory contributions to the level density associated with classical closed orbits. These orbits form families as in integrable systems, and so their contribution is of order $E^{-1/4}$ rather than the $E^{-1/2}$ characteristic of isolated orbits. But in contrast with integrable systems the families fill only part of their invariant surfaces.

Acknowledgement

We thank Dr. J.H. Hannay for many helpful discussions. This research was not supported by any military agency.

Appendix A

Algebraic technique for calculating the genus of invariant phase-space surfaces

This is based on the well-known result [8] that the genus g of a surface is given in terms of the number of faces (F), edges (E) and vertices (V) in any polygonalization by the formula

$$2-2g=F-E+V. \tag{A.1}$$

For the $\pi/3$ rhombus, the polygonalization of fig. 1d yields $F=6$, $E=12$, $V=4$, so that $g=2$ as already obtained in section 2. For the square torus billiard, the polygonalization of fig. 2b yields $F=4$ and $E=16$, and there are four external vertices and four internal vertices, so that $V=8$; therefore (A.1) gives $g=5$ as in section 2. Finally, for the desymmetrized square torus billiard the polygonalization of fig. 5 gives $F=8$, $E=16$, $V=6$, so that $g=2$.

Appendix B

Quantization of $\pi/3$ rhombus

This is the simplest pseudointegrable system we know of. Quantum-mechanically, its eigenfunctions (solutions of (11)), must have either even or odd symmetry about the short diagonal (fig. 14). The odd solutions are formed by juxtaposing solutions for the equilateral triangle with Dirichlet boundary conditions, and we begin by discussing these.

The equilateral triangle is an integrable system with three natural circuits on its torus (fig. 1b); any two of these are independent. If the triangle has unit side length, the actions (6) round these circuits are

$$I_1=-\frac{3p_x}{4\pi}+\frac{\sqrt{3}p_y}{4\pi},\ I_2=+\frac{3p_x}{4\pi}+\frac{\sqrt{3}p_y}{4\pi},\ I_3=\frac{\sqrt{3}p_y}{2\pi}. \tag{B.1}$$

Quantizing any pair of these as integer multiples m, n of Planck's constant leads to energy levels

$$k^2=\frac{16\pi^2}{9}(m^2+n^2-mn), \tag{B.2}$$

and enables twelve plane waves to be constructed [20]. By combining these waves into functions that vanish on two sides $y=\pm\sqrt{3}x$ of the triangle, we obtain doubly degenerate

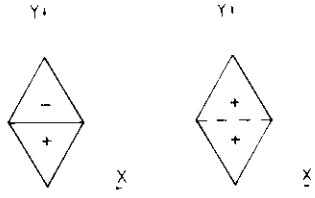

Fig. 14. Odd and even states of the $\pi/3$ rhombus; ψ vanishes on the full lines, and $\nabla\psi$ vanishes across the dashed line.

eigenfunctions $\psi^{c}_{m,n}$ and $\psi^{s}_{m,n}$ that also vanish on the third side $y = \sqrt{3}/2$, namely

$$\psi^{s,c}_{m,n} = \begin{pmatrix}\sin\\ \cos\end{pmatrix}\left\{\frac{2\pi}{3}(2m-n)x\right\}\sin\left\{\frac{2\pi n y}{\sqrt{3}}\right\} - \begin{pmatrix}\sin\\ \cos\end{pmatrix}\left\{\frac{2\pi}{3}(2n-m)x\right\}\sin\left\{\frac{2\pi m y}{\sqrt{3}}\right\} + \begin{pmatrix}\sin\\ \cos\end{pmatrix}\left\{-\frac{2\pi}{3}(m+n)x\right\} \times \sin\left\{\frac{2\pi(m-n)y}{\sqrt{3}}\right\}. \tag{B.3}$$

By differentiation, it is easy to show that these waves satisfy Schrodinger's equation with the enegies (B.2), so that the 'WKB' construction yields the exact eigenfunctions for this case. Some of the lower-lying states are illustrated in fig. 15. The states satisfy the relations

$$\psi^{c,s}_{n,m} = -\psi^{c,s}_{m,n}; \quad \psi^{c}_{m,m-n} = \psi^{c}_{m,n}, \quad \psi^{s}_{m,m-n} = -\psi^{s}_{m,n},$$

$$\psi^{c}_{-m,-n} = -\psi^{c}_{m,n}, \quad \psi^{s}_{-m,-n} = +\psi^{s}_{m,n}. \tag{B.4}$$

These relations can be employed in conjunction with the elliptical form of the constant-energy contours in (m, n) space to show that the smoothed mode number is

$$\overline{\mathcal{N}}(k) = \frac{\sqrt{3}k^2}{16\pi}. \tag{B.5}$$

Weyl's area rule gives exactly the same result, thus confirming that the solutions (B.3) exhaust the set of eigenfunctions of the equilateral triangle.

Turning now to the $\pi/3$ rhombus, the same area rule indicates that the states (B.3) constitute exactly half the eigenfunctions. The other half, even under reflection about the short diagonal (fig. 14), are obtained by juxtapositioning solutions for the equilateral triangle in which two edges have Dirichlet boundary conditions and one side has Neumann conditions. But such solutions cannot be constructed by superposing

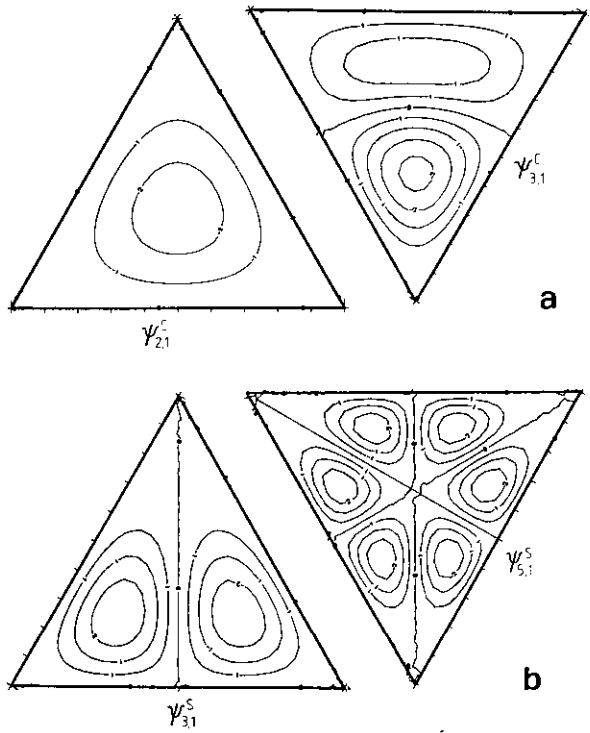

Fig. 15. Contours of ψ for some eigenfunctions (B.3) of the equilateral triangle.

plane waves as in (B.3), because (B.3), with a linear scaling of x and y, are in fact the only such superpositions vanishing on the lines $y = \pm\sqrt{3}x$, and their gradients $\partial/\partial y$ do not vanish along any lines y = constant. As corroborative evidence we note that the phase-space surface of the triangle with one Neumann edge (fig. 16) does not admit of 'torus' quantization because there exist two equivalent circuits ((i) and (ii)) whose bounce numbers would give rise to different phases ((i) has one Neumann and three

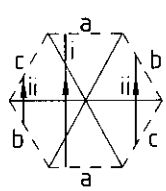

Fig. 16. Phase space surface for triangle with one Neumann edge (dashed line) and two Dirichlet edges (full line), together with two equivalent circuits (i) and (ii).

Dirichlet reflections, while (ii) has two reflections of each type).

We conclude that in quantum mechanics the pseudointegrability of the $\pi/3$ rhombus manifests itself in the 'even' eigenfunctions, whose plane-wave expansion must presumably involve infinitely many evanescent contributions, as with the square torus billiard of section 3.

Appendix C

Effect of boundary conditions on the spectrum of the $\pi/4$ right triangle

Let the triangle have unit base and height. Elementary combinations of plane-wave solutions of Schrödinger's equation gives the energy levels, in terms of the variable (20) as

$$\mathscr{E} = m^2 + n^2,$$

where

$1 \leqslant n < m$, for Dirichlet boundary conditions (D),
$0 \leqslant n \leqslant m$, for Neumann boundary conditions (N). (C.1)

The level density is therefore

$$d_{\mathrm{D,N}}(\mathscr{E}) = \sum_{A_{\mathrm{D,N}}} \sum (\mathscr{E} - m^2 - n^2), \qquad \text{C.2)}$$

where A_{D} and A_{N} are summation domains in the m, n, plane (fig. 17) which respectively exclude and include the lines of lattice points along the x-axis and diagonal.

This system is integrable, and so the procedure for obtaining the semiclassical approximation to $d(\mathscr{E})$ is to replace the sum in (C.2) by a sum of integrals over the domain A_{D} or A_{N} in the plane $\boldsymbol{\mu} \equiv (m, n)$, using the Poisson formula [7]. We shall integrate over the domain A consisting of a $\pi/4$ sector (fig. 17) which will give the mean of the Neumann and Dirichlet level densities. Thus

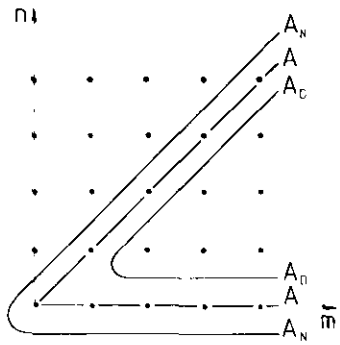

Fig. 17. Lattice of quantum numbers m, n for the $\pi/4$ right triangle, showing the boundaries of the sectors A_{D} and A_{N} contributing in the case of Dirichlet and Neumann boundary conditions, and the sector A contributing to the average level density $(d_{\mathrm{D}} + d_{\mathrm{N}})/2$.

$$\frac{d_{\mathrm{D}}(\mathscr{E}) + d_{\mathrm{N}}(\mathscr{E})}{2} = \sum_{\boldsymbol{M}} \sum \int_{A} \int \mathrm{d}\mu \delta(\mathscr{E} - \mu^2)\, \mathrm{e}^{2\pi \mathrm{i} \boldsymbol{M} \cdot \boldsymbol{\mu}}, \qquad \text{(C.3)}$$

where $\boldsymbol{M}$ is a vector in the dual lattice of integers. In polar coordinates (μ, ϕ) and (M, ϕ_M), the μ integration is trivial and gives

$$\frac{d_{\mathrm{D}}(\mathscr{E}) + d_{\mathrm{N}}(\mathscr{E})}{2} = \frac{\pi}{8} + \frac{1}{2} \sum_{M} \sum{}' \int_{0}^{\pi/4} \mathrm{d}\phi \times \exp\{2\pi i M \sqrt{\mathscr{E}} \cos(\phi - \phi_M)\}, \qquad \text{(C.4)}$$

where the prime means that $\boldsymbol{M} = 0$ is excluded. The term $\pi/8$ is the steady 'Weyl' density for this case, and the terms in the sum give the oscillations.

Under semiclassical conditions, i.e. as $\mathscr{E} \to \infty$, the phases in the ϕ integrals oscillate rapidly, and so the principle of stationary phase can be employed. Stationary points occur when $\phi = \phi_M$ and $\phi = \phi_M + \pi$, so that

$$\frac{d_{\mathrm{D}}(\mathscr{E}) + d_{\mathrm{N}}(\mathscr{E})}{2} \approx \frac{\pi}{8} + \mathrm{Re} \sum_{M} \sum{}' \exp\{2\pi \mathrm{i} M \sqrt{\mathscr{E}}\} \times \int_{0}^{\pi/4} \mathrm{d}\phi \exp\{\mathrm{i}\pi M \sqrt{\mathscr{E}} (\phi - \phi_M)^2\}. \qquad \text{(C.5)}$$

The integrals are of Fresnel type, and their behaviour as $\mathscr{E} \to \infty$ depends on whether M lies within, on or outside the 45° sector A on fig. 17 (now imagined as a picture of the M plane rather than the μ plane), with the result

$$\frac{d_D(\mathscr{E}) + d_N(\mathscr{E})}{2} \approx \frac{\pi}{8} + \mathscr{E}^{-1/4} \sum_M {\sum}' \frac{\beta_M}{\sqrt{M}} \times \cos\left\{2\pi M\sqrt{\mathscr{E}} - \frac{\pi}{4}\right\}$$

where

$$\beta_M = \begin{cases} 1, & \text{if } 0 < \phi_M < \frac{\pi}{4} \\ \frac{1}{2}, & \text{if } \phi_M = 0, \quad \text{or} \quad \phi_M = \frac{\pi}{4}, \\ 0, & \text{otherwise.} \end{cases} \qquad \text{(C.6)}$$

This is precisely the closed path sum (30), derived in section 5 by the Green function method: for the $\pi/4$ triangle, closed paths are generated by trajectories with rational directions, labelled by M; the length of the M-path is $2M$ and it fills the phase-space invariant surface, which in this case has eight sheets each with area 1/2. The paths for which $\beta_M = \frac{1}{2}$ are those hitting a side of the triangle perpendicularly: they retrace themselves and so are not topologically distinct when described in the reverse sense, as is the case with all the other closed paths.

To discriminate between Dirichlet and Neumann boundary conditions it is necessary to include explicitly a sum over the 'boundary' lattice points in (C.2), i.e. to evaluate

$$d_N(\mathscr{E}) - d_D(\mathscr{E}) \equiv \Delta d(\mathscr{E}) = \sum_{n=0}^{\infty} \epsilon_n \{\delta(\mathscr{E} - n^2) + \delta(\mathscr{E} - 2n^2)\}$$

$$(\epsilon_n = 1, \quad \text{if } n > 0, \quad \epsilon_n = \tfrac{1}{2}, \quad \text{if } n = 0). \qquad \text{(C.7)}$$

Applied to this one-dimensional summation, the Poisson formula gives the exact result

$$\Delta d(\mathscr{E}) = \frac{(1 + 1/\sqrt{2})\mathscr{E}^{-1/2}}{2} + \mathscr{E}^{-1/2} \sum_{M=1}^{\infty} \left[\cos(2\pi N\sqrt{\mathscr{E}}) + \frac{1}{\sqrt{2}} \cos(\pi M\sqrt{(2\mathscr{E})})\right]. \qquad \text{(C.8)}$$

The first term gives the edge correction to the steady 'Weyl' density for this case, with the

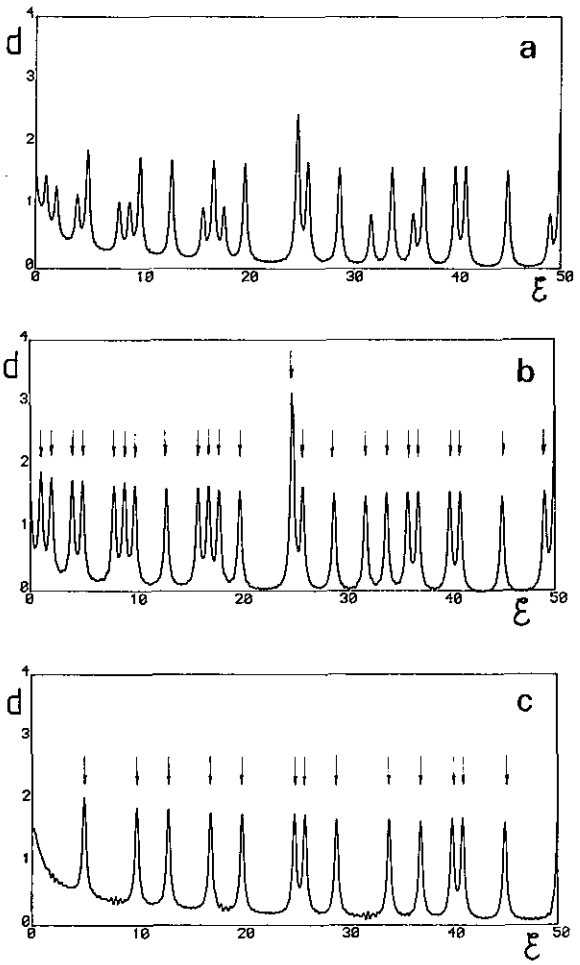

Fig. 18. Semiclassical closed path sums for $\pi/4$ right triangle with smoothing width (imaginary part of energy) $\delta = 0.2$; (a) average of $d(\mathscr{E})$ for Neumann and Dirichlet boundary conditions, eq. (C.6); (b) with correction $+\Delta d/2$, eq. (C.8), for Neumann conditions; (c) with correction $-\Delta d/2$, eq. (C.8), for Dirichlet conditions. Positions of the exact quantum levels are marked with arrows.

correct magnitude and sign [10] to discriminate between Dirichlet and Neumann boundary conditions. The oscillatory terms come from the closed orbits that graze the sides of the triangle, and are of lower order in $\mathscr{E}$ than the corresponding terms in (C.6).

Fig. 18 shows computations of $d(\mathscr{E})$ according to the 'uncorrected' semiclassical formula (C.6) and with $\Delta d/2$ (eq. (C.8)) added and subtracted All densities are smoothed, corresponding to complex energies $\mathscr{E} + i0.2$. It is easy to see how Neumann boundary conditions introduce extra states, and how the uncorrected formula interpolates between the two cases.

Note added in proof

Professor J. Ford has kindly drawn our attention to ref. [22], in which it is shown that rational billiard motion is typically dense on the invariant surfaces.

References

[1] V.I. Arnol'd, Mathematical Methods of Classical Mechanics (Springer, New York, 1978).
[2] M.V. Berry, Regular and Irregular Motion, in Topics in Non-Linear Mechanics, S. Jorna, Ed., Am. Inst. Phys. Conf. Proc. 46 (1978) 16.
[3] A. Einstein, Verhandl. Deut. Phys. Ges. 19 (1917) 82.
[4] M.V. Berry, Ann. Phys., in press, 1981.
[5] M.C. Gutzwiller, J. Math. Phys. 8 (1967) 1979, 10 (1969) 1004, 11 (1970) 1791, 12 (1971) 343.
[6] R. Balian and C. Bloch, Ann. Phys. 69 (1972) 76, 85 (1974) 514.
[7] M.V. Berry and M. Tabor, Proc. Roy. Soc. A349 (1976) 101.
[8] B.R. Pollard, Introduction to Algebraic Topology, to be published.
[9] Ya. G. Sinai, Russ. Math. Surv. 25 (1970) 137 (No. 2).
[10] H.P. Baltes and E.R. Hilf, Spectra of Finite Systems (B-I Wissenschaftsverlag, Mannheim, 1978).
[11] M.V. Berry and K.E. Mount, Rep. Progr. Phys. 35 (1972) 315.
[12] M.V. Berry and M. Tabor, J. Phys. A. 10 (1977) 371.
[13] I.C. Percival, J. Phys. B.6 (1973) L229.
[14] J. Von Neumann and E.P. Wigner, Physik. Z. 30 (1929) 467.
[15] S.W. McDonald and A.N. Kaufman, Phys. Rev. Lett. 42 (1979) 1189.
[16] M.V. Berry and M. Tabor, Proc. Roy. Soc. A356 (1977) 375.
[17] M. Abramowitz and I.A. Stegun, Handbook of Mathematical Functions (U.S. National Bureau of Standards, Washington, DC, 1964).
[18] M.C. Gutzwiller, J. Math. Phys., 18 (1977) 806.
[19] M.C. Gutzwiller, Phys. Rev. Lett. 45 (1980) 150.
[20] J.B. Keller and S.I. Rubinow, Ann. Phys. (New York) 9 (1960) 24.
[21] A. Hobson, J. Math. Phys. 16 (1975) 2210.
[22] A.N. Zemlyakov and A.B. Katok, Mat. Zametki. 18 (1975) 291 (English translation: Math. Notes 18 (1976) 760).